Dual-Band LFM Signal Generation by Optical Frequency Quadrupling and Polarization Multiplexing

Qingshui Guo, Fangzheng Zhang, *Member, IEEE*, Pei Zhou, and Shilong Pan, *Senior Member, IEEE*

***Abstract*— A photonic approach to generating dual-band linear frequency modulation (LFM) signal is proposed based on optical frequency quadrupling and polarization multiplexing. This is achieved by using an integrated polarization multiplexing dual-parallel Mach–Zehnder modulator to perform frequency quadrupling in two orthogonal polarizations independently. After optical-to-electrical conversion, two LFM signals in different frequency bands can be generated simultaneously. The proposed scheme has a very simple and compact structure. Thanks to the frequency quadrupling technique, high-frequency, and wideband LFM signals can be generated with low speed electrical devices. The central frequency, bandwidth, and temporal duration of the generated LFM signals can be easily adjusted. In the experiment, the generation of dual-band LFM signals in K-band and Ka-band (centered at 20 and 30 GHz, respectively) is demonstrated. Tunability of the central frequency, bandwidth, and time duration is also verified. The proposed signal generator is a promising candidate in dual-band multi-function radar applications.**

***Index Terms*— Linear frequency modulation (LFM), microwave photonics, polarization multiplexing.**

I. Introduction

MODERN radar systems are requiring increasingly multiple functionalities and high performance to provide a complete cognition of the targets. To achieve this goal, it is important to collect a great variety of information [1]. A dual-band radar can satisfy this requirement thanks to the use of two frequency bands [2]. Compared with a single-band radar, a dual-band radar can increase the detection probability of small targets, expand the detection range and improve the range resolution by data fusion of two frequency bands [3], [4]. On the other side, linear frequency modulation (LFM) signals, with very good pulse compression capability, are widely used to achieve a large detection range and a high range resolution [5], [6]. Therefore, a dual-band radar with LFM signals possess both the excellent features originated from a dual-band system and LFM technique. A fully coherent dual-band photonic-assisted radar has been demonstrated in real aerial targets detection, which achieved both good resolution and good sensitivity by data fusion of two LFM signals in S-band and X-band [7]. Traditionally, LFM signals are generated in electrical domain using a voltage-controlled oscillator [8] or a direct digital synthesizer (DDS) [9]. The generated signals have limitations of low frequency and small bandwidth (usually less than a few GHz), which are not competent in advanced high performance radar systems requiring LFM signals with a large time bandwidth product (TBWP) [10], [11]. To increase the frequency and bandwidth, multiple stages of electrical frequency multiplication can be applied. However, the system is usually complicated with multiple band pass filters and amplifiers, and there is also considerable challenges in impedance matching [9]. To address these problems, microwave photonic technologies have been investigated extensively to generate high-frequency and wideband signals [12]–[14]. One such method is realized by optical spectral shaping with frequency-to-time mapping [12], [13]. This method can generate LFM signal with a bandwidth up to tens of gigahertz, but due to the use of free-space optical devices, the system is complicated and suffers from large size and high coupling loss. Another photonic-assisted LFM signal generation method is achieved by heterodyning a chirped optical pulse with a continuous wave (CW) light or another linearly chirped optical pulse with different chirp rate [14], [15]. The major limitation with this method is the small time aperture (usually several or tens of nanoseconds) that prevents its applications. Previous studies are mainly focused on the generation of a single-band LFM signal. Photonic method for dual-band LFM signal generation has been rarely reported. To the best of our knowledge, the only method in literature is realized by microwave photonic frequency up-conversion of two electrical intermediate frequency LFM signals using a mode locking laser and an electro-optical modulator [7]. In this method, central frequency of the generated signal can be very high, but the signal bandwidth is strictly limited by the repetition rate of a passively mode locked laser.

In this letter, we propose a photonic approach to generating dual-band LFM signal based on optical frequency quadrupling and polarization multiplexing. The system is very simple applying an integrated electro-optical modulator, without any optical filters or other optical signal processing module.

Manuscript received April 25, 2017; revised June 1, 2017; accepted June 27, 2017. Date of publication June 30, 2017; date of current version July 19, 2017. This work was supported in part by the NSFC Program under Grant 61401201 and Grant 61422108, in part by the NSFC Program of Jiangsu Province under Grant BK20140822, and in part by the open fund of Science and Technology on Monolithic Integrated Circuits and Modules Laboratory under Grant 20150C1404. *(Corresponding authors: Fangzheng Zhang; Shilong Pan.)*

The authors are with the Key Laboratory of Radar Imaging and Microwave Photonics, Ministry of Education, Nanjing University of Aeronautics and Astronautics, Nanjing 210016, China (e-mail: zhangfangzheng@nuaa.edu.cn; pans@ieee.org).

Color versions of one or more of the figures in this letter are available online at http://ieeexplore.ieee.org.

Digital Object Identifier 10.1109/LPT.2017.2722004

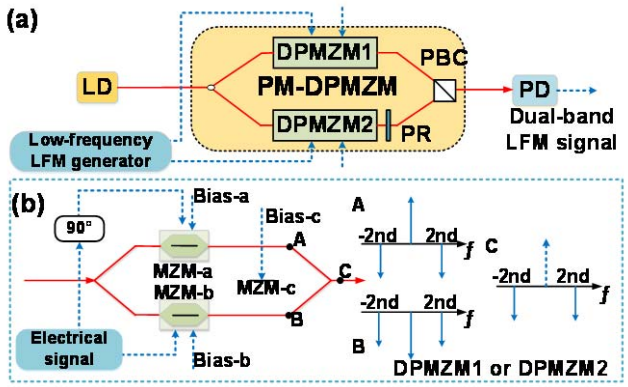

Fig. 1. (a) Schematic diagram of the proposed signal generator and (b) illustration of the operation principle in each DPMZM. LD: laser diode; PBC: polarization beam combiner; PR: polarization rotator; PD: photodetector; MZM: Mach-Zehnder modulator.

It generates two LFM signals in different frequency bands along two optical polarization states. The frequency quadrupling technique makes it possible to generate high- frequency and wideband LFM signals with low-speed electronics. The system is also reconfigurable since the central frequency, bandwidth and time duration of the generated LFM signals can be easily adjusted. An experiment is carried out to verify the feasibility of the proposed scheme. The tunability of the generated LFM signals is also experimentally investigated.

II. Principle

Fig. 1 shows the schematic diagram of the proposed dual-band frequency-quadrupled LFM signal generator. A continuous wave (CW) light from a laser diode (LD) is coupled into a PM-DPMZM, which is an integrated device consisting of two DPMZMs (DPMZM1 and DPMZM2), a polarization rotator (PR) and a polarization beam combiner (PBC). Each DPMZM has two sub-MZMs (MZM-a and MZM-b) embedded in one of the two arms of a main MZM (MZM-c). The light fed to the PM-DPMZM is equally split into two branches and the light in each branch is sent to a DPMZM. The two DPMZMs work in a frequency quadrupling mode. In this scheme, an electrical signal from a low-frequency LFM signal is applied to drive DPMZM1 and DPMZM2, respectively. As shown in Fig.1 (b), the electrical signal is split into two parts with a phase difference of 90 degree and applied to drive the two sub-MZMs, respectively. By biasing MZM-a and MZM-b at their maximum transmission points, a serial of even-order sidebands are generated. After properly choosing the amplitude of the driving signals, only the optical carrier and the $\pm 2^{\text{nd}}$-order sidebands dominate considering the higher sidebands have a very small amplitude. MZM-c is biased at the minimum transmission point to suppress the optical carrier [16]. At the output of each DMPZM, only the $\pm 2^{\text{nd}}$-order sidebands are obtained. After that, the polarization of the signal in the lower branch of the PM-DPMZM is rotated by 90 degree through the PR. Thus, a pair of orthogonally polarized optical signal we obtain in the two branches of the PM-DPMZM. After they are combined by the PBC, a polarization-multiplexed optical signal is obtained at the output of the PM-DPMZM. When this optical signal is sent to a photodetector (PD), optical-to-electrical conversion can be performed in the two polarizations without interference between each other. After the PD, two frequency-quadrupled LFM signals (compared with the driving signals) are generated simultaneously, of which the bandwidths are also quadrupled. To get dual-band LFM signal, the electrical signals driving the two DMPMZMs should be spectrally separated. In this method, the central frequency and bandwidth of generated signal is four times that of the deriving signals, indicating the capability of generating high-frequency and wideband LFM signals with low speed electric devices. Besides, the central frequency, bandwidth and time duration of the generated LFM signal can be easily adjusted by changing the low-speed electrical signals driving the DPMZMs.

III. Experiment Results and Discussion

To verify the feasibility of the proposed system, an experiment is implemented based on the setup in Fig. 1. A linearly polarized light wave at 1550.11 nm with a power of 14.0 dBm from a LD (TeraXion) is sent to a PM-DPMZM (Fujitsu DP-TM79HQA), which has a 3-dB bandwidth of 23 GHz and a half-wave voltage of 3.5 V @ 23 GHz. An arbitrary waveform generator (AWG Tektronix AWG70001) with a maximum sampling rate of 50 GSa/s is applied to generate two electrical LFM signals centered at 7.5 GHz and 5 GHz, respectively. The two LFM signals, both having a bandwidth of 1 GHz and a time duration of 1μs, are properly amplified and passed through two 90 degree hybrids (bandwidth: 2-18 GHz), before applied to DPMZM1 and DPMZM2, respectively. After carefully adjusting the amplitudes of the driving signals and the bias voltages, optical carrier-suppressed $\pm 2^{\text{nd}}$-order sidebands signals are generated in each branch of the PM-DPMZM. Following the PM-DPMZM, a PD (u2t XPDV2120R-VF-FP) with a band- width of 59 GHz and a sensitivity of 0.6 A/W is used to perform optical-to-electrical conversion. The waveform of the generated dual-band LFM signal is observed using a real time oscilloscope (Agilent DSO-X 92504A) with a sampling rate of 80GSa/s, as show in Fig. 2 (a). The electrical spectrum of this signal is measured by an electrical signal analyzer (Rohde & Schwarz FSV40), as shown in Fig. 2(b), and the instantaneous frequency-time diagram is shown in Fig. 2 (c), which is obtained by applying short-time Fourier transformation to the waveform in Fig. 2(a). As can be seen, a dual-band LFM signal (18-22 GHz, 28-32 GHz) with a time duration of 1 μs is generated. Both the central frequency and bandwidth is quadrupled compared with the driving signal. In practical applications, it is usually necessary to separate the LFM signals in different bands before applied to different transceivers, which can be easily achieved by applying certain electrical filters. In our experiment, to separate the LFM signals in Fig. 2, a Ka-band (26.5-40 GHz) filter and a K-band (18-26.5 GHz) filter are applied after the PD. Fig. 3 (a) shows the waveform of the LFM signal in Ka-band, of which the instantaneous frequency-time diagram is shown in Fig. 3 (b). A signal centered at 30 GHz with bandwidth

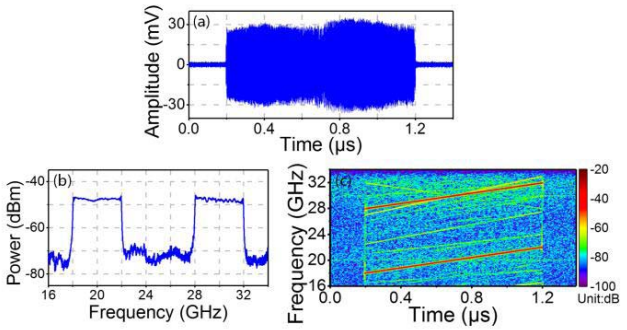

Fig. 2. (a) Waveform of the generated dual-band LFM signal, (b) electrical spectrum of the dual-band LFM signal, and (c) the calculated instantaneous frequency-time diagram (18-22 GHz, 28-32 GHz).

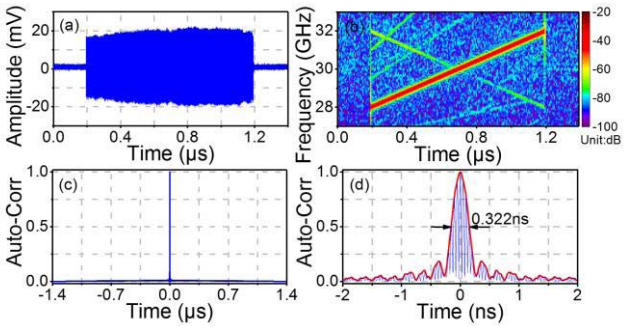

Fig. 3. (a) Waveform of the generated Ka-band LFM signal, (b) the calculated instantaneous frequency-time diagram (28-32 GHz), (c) the calculated auto-correlation result, and (d) zoom-in view of the auto-correlation peak (red line curve is the fitted envelope).

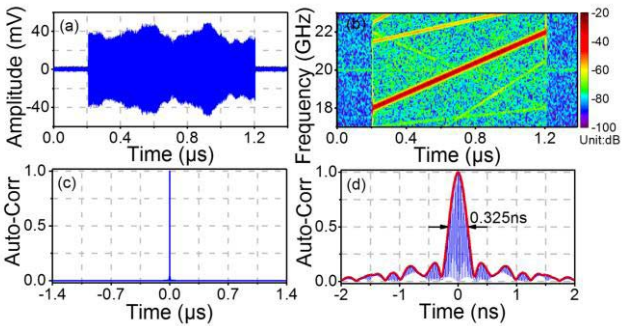

Fig. 4. (a) Waveform of the generated K-band LFM signal, (b) the calculated instantaneous frequency-time diagram (18-22 GHz), (c) the calculated auto-correlation result, and (d) zoom-in view of the auto-correlation peak (red line curve is the fitted envelope).

4 GHz and pulse width 1 μs can be seen, corresponding to a TBWP of 4000. To check the pulse compression capability, auto-correlation is calculated, as shown in Fig. 3 (c), where a narrow peak is clearly observed. Fig. 3 (d) shows the zoom-in view of the auto- correlation peak, of which the full-width at half maximum (FWHM) is about 0.322 ns. Fig. 4 shows the results of the generated LFM signal in K-band. The temporal waveform with a pulse width of 1 μs is shown in Fig. 4 (a). The calculated instantaneous frequency-time diagram is shown in Fig. 4 (b) with a center frequency of 20 GHz and a bandwidth of 4 GHz. The TBWP of the K-band LFM signal is also 4000. Fig. 4 (c) and (d) show the auto-correlation results. The FWHM of the compressed pulse is about 0.325 ns.

In the proposed system, an important issue is the cross-talk between the LFM signals in different bands due to the

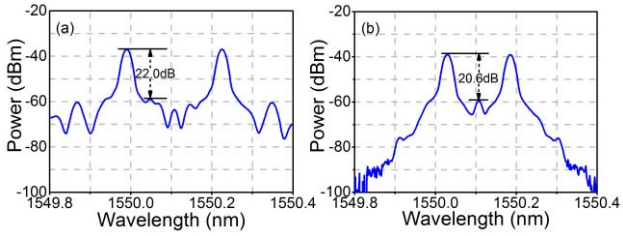

Fig. 5. (a) Optical spectrum of the single in X polarization, and (b) optical spectrum of the signal in Y polarization.

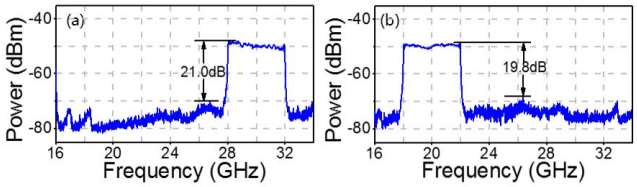

Fig. 6. (a) Electrical spectrum of the Ka-band LFM signal (28-32 GHz) obtained from X polarization, and (b) electrical spectrum of the K-band LFM signal (18-22 GHz) obtained from Y-polarization.

possible_cross-talk between the two polarizations. To investigate this property, a polarization controller and a polarization beam splitter are connected after the PM-DPMZM to extract the signal in each polarization. The optical spectrum in each polarization is shown in Fig. 5, which is measured by an optical spectrum analyzer (YOKOGAWA AQ6370C) with a resolution of 0.02 nm. Fig. 5 (a) is the optical spectrum in X polarization, where the two second-order sidebands are 22.0 dB higher than the unwanted optical sidebands. Fig. 5 (b) is the optical spectrum in Y polarization, with the power of the two second-order sidebands 20.6 dB higher than that of the optical carrier. Then, the two optical signals are sent to a PD, respectively. Two separate LFM signals in different frequency bands are obtained. Fig. 6 (a) shows the electrical spectrum of the Ka-band signal (28-32 GHz) generated from X polarization, where the signal power is 21.0 dB higher than the undesired frequency components. Fig. 6 (b) is the spectrum of the K-band signal (18-22 GHz) obtained from Y polarization. The unwanted frequency components are suppressed by 19.8 dB. The results in Fig. 6 indicate that there is no obvious cross-talk between the two LFM signals.

The previous results can confirm the feasibility of the proposed dual-band LFM signal generator with frequency quadrupling capability. Another property of the proposed system is that the generated LFM signal can be easily reconfigured to have different central frequency, bandwidth and temporal duration. This is achieved by properly setting the output signals from the low-speed AWG. To check the bandwidth tunability, the LFM signal applied to DPMZM1 is still centered at 7.5 GHz with a time duration of 1 μs, but the signal bandwidth is changed to 0.1 GHz. The generated LFM signal is still centered at 30 GHz, but the bandwidth is 0.4 GHz (29.8-30.2 GHz), as shown by the instantaneous frequency-time diagram in Fig. 7 (a). In Fig. 7 (b), The FWHM of the compressed pulse is 3.14 ns. When the central frequency of the input electrical LFM signal is changed to 2.5 GHz, while the bandwidth is 1 GHz and the time duration is 1 μs,

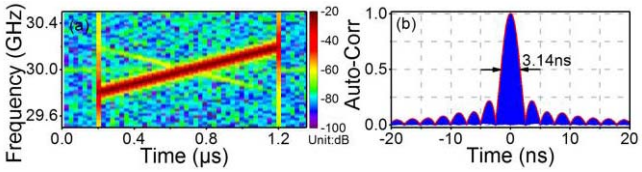

Fig. 7. (a) The instantaneous frequency-time diagram of the generated LFM signal centered at 30 GHz with a time duration of 1 μs and a bandwidth of 0.4 GHz, (b) the zoom-in view of auto-correlation peak.

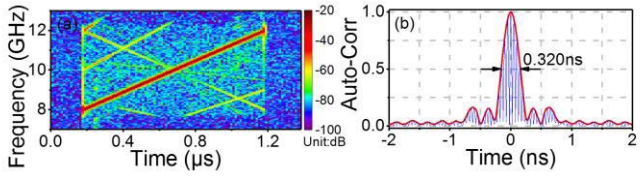

Fig. 8. (a) The instantaneous frequency-time diagram of the generated LFM signal centered at 10 GHz with a time duration of 1 μs and a bandwidth of 4 GHz, (b) the zoom-in view of auto-correlation peak.

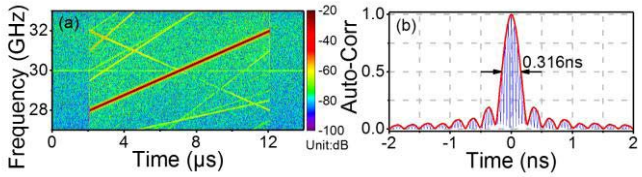

Fig. 9. (a) The instantaneous frequency-time diagram of the generated LFM signal centered at 30 GHz with a time duration of 10 μs and a bandwidth of 4 GHz, (b) the zoom-in view of auto-correlation peak.

an X-band LFM signal centered at 10 GHz with a bandwidth of 4 GHz is generated. Fig. 8 shows the measured results. As shown in Fig. 8 (a), the instantaneous frequency changes for 8 GHz to 12 GHz, and the TBWP is 4000. The FWHM of the compressed pulse is about 0.320 ns. Fig. 9 shows the experimental results when changing the pulse duration to 10 μs. In this case, the low-frequency LFM signal from the AWG is centered at 7.5 GHz with a bandwidth of 1 GHz. As shown in Fig. 9 (a) a LFM signal from 28 GHz to 32 GHz is generated with a temporal duration of 10 μs. The TBWP is increased to 40000. After pulse compression, the FWHM of the compressed pulse is 0.316 ns, as shown in Fig.9 (b). Thus, the reconfigurable property of the proposed signal generator is also verified.

IV. Discussion and Conclusion

In the experimental results, very weak harmonic signals are observed in the frequency-time diagram. The main reason is that the undesired modulation sidebands during frequency quadrupling are not totally removed. This problem can be solved by strictly controlling the bias voltages and the driving signal amplitudes to achieve a better power suppression ratio between $\pm 2^{nd}$ order and the other unwanted sidebands. Since the low-frequency LFM signals from an AWG can have very good phase coherence. After frequency quadrupling, this property can be preserved. Thus, the generated dual-band LFM signals are possible to be used in coherent dual-band radar systems.

In conclusion, we have proposed and demonstrated a dual-band LFM signal generator for applications in dual-band radar systems. The proposed scheme is based on optical frequency quadrupling and polarization multiplexing. It has a very simple structure using an integrated electro-optical modulator. Simultaneous generation of dual-band LFM signals are experimentally implemented. The tunable capability of the central frequency, bandwidth and time duration is also demonstrated.

References

[1] M. Vespe, C. J. Baker, and H. D. Griffiths, "Automatic target recognition using multi-diversity radar," *IET Radar Sonar Navigat.*, vol. 1, no. 6, pp. 470–478, 2007.

[2] P. Van Dorp, R. Ebeling, and A. G. Huizing, "High resolution radar imaging using coherent multiband processing techniques," in *Proc. IEEE Radar Conf.*, Apr. 2010, pp. 981–986.

[3] J. Tian, J. Sun, G. Wang, Y. Wang, and W. Tan, "Multiband radar signal coherent fusion processing with IAA and apFFT," *IEEE Signal Process. Lett.*, vol. 20, no. 5, pp. 463–466, May 2013.

[4] J. Han and C. Nguyen, "Development of a tunable multiband UWB radar sensor and its applications to subsurface sensing," *IEEE Sonsors J.*, vol. 7, no. 1, pp. 51–58, Jan. 2007.

[5] W. L. Melvin and J. A. Scheer, *Principles of Modern Radar: Advanced Techniques*. Herts, U.K.: SciTech, 2014.

[6] F. Gini, A. De Maio, and L. Patton, *Waveform Design and Diversity for Advanced Radar Systems*. London, U.K.: Institution of Engineering and Technology, 2012.

[7] P. Ghelfi, F. Laghezza, F. Scotti, D. Onori, and A. Bogoni, "Photonics for radars operating on multiple coherent bands," *J. Lightw. Technol.*, vol. 34, no. 2, pp. 500–507, Jan. 15, 2015.

[8] H. Kwon and B. Kang, "Linear frequency modulation of voltage-controlled oscillator using delay-line feedback," *IEEE Microw. Wireless Compon. Lett.*, vol. 15, no. 6, pp. 431–433, Jun. 2005.

[9] Q. H. Li, D. Yang, X. H. Mu, and Q. L. Huo, "Design of the L-band wideband LFM signal generator based on DDS and frequency multiplication," in *Proc. Int. Conf. Microw. Millim. Wave Technol. (ICMMT)*, May 2012, pp. 1–4.

[10] T. Musch, "A high precision 24-GHz FMCW radar based on a fractional-N ramp-PLL," *IEEE Trans. Instrum. Meas.*, vol. 52, no. 2, pp. 324–327, Apr. 2003.

[11] N. Pohl *et al.*, "Radar measurements with micrometer accuracy and nanometer stability using an ultra-wideband 80 GHz radar system," in *Proc. IEEE Topical Conf. Wireless Sensors Sensor Netw. (WiSNet)*, Jan. 2013, pp. 31–33.

[12] I. S. Lin, J. D. McKinney, and A. M. Weiner, "Photonic synthesis of broadband microwave arbitrary waveforms applicable to ultra-wideband communication," *IEEE Microw. Wireless Compon. Lett.*, vol. 15, no. 4, pp. 226–228, Apr. 2005.

[13] C. Wang and J. P. Yao, "Chirped microwave pulse generation based on optical spectral shaping and wavelength-to-time mapping using a Sagnac loop mirror incorporating a chirped fiber Bragg grating," *J. Lightw. Technol.*, vol. 27, no. 16, pp. 3336–3341, Aug. 15, 2009.

[14] H. Gao, C. Lei, M. Chen, F. Xing, H. Chen, and S. Xie, "A simple photonic generation of linearly chirped microwave pulse with large time-bandwidth product and high compression ratio," *Opt. Exp.*, vol. 21, no. 20, pp. 23107–23115, Oct. 2013.

[15] H. Zhang, W. Zou, and J. Chen, "Generation of a widely tunable linearly chirped microwave waveform based on spectral filtering and unbalanced dispersion," *Opt. Lett.*, vol. 40, no. 6, pp. 1085–1088, 2015.

[16] C. T. Lin, P. T. Shih, J. Chen, W. Q. Xue, P. C. Peng, and S. Chi, "Optical millimeter-wave signal generation using frequency quadrupling technique and no optical filtering," *IEEE Photon. Technol. Lett.*, vol. 20, no. 12, pp. 1027–1029, Jun. 15, 2008.